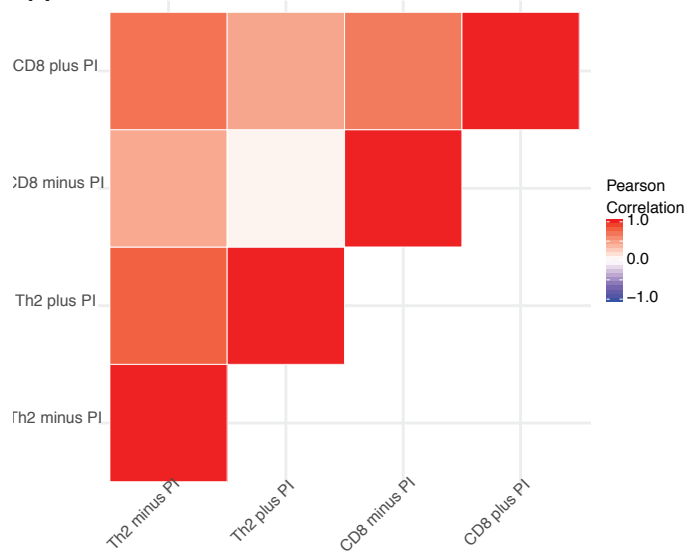
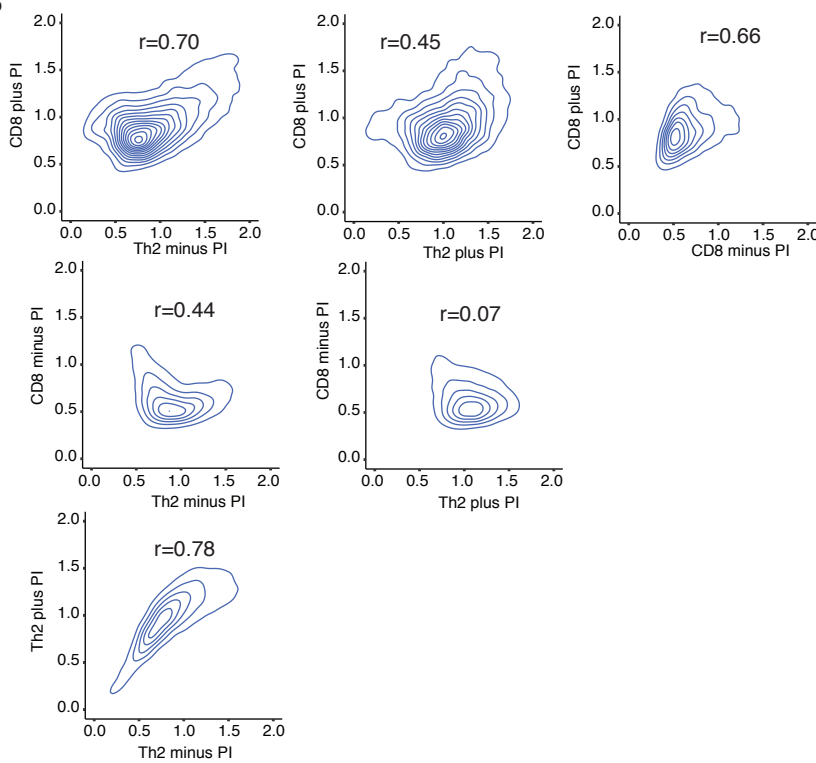
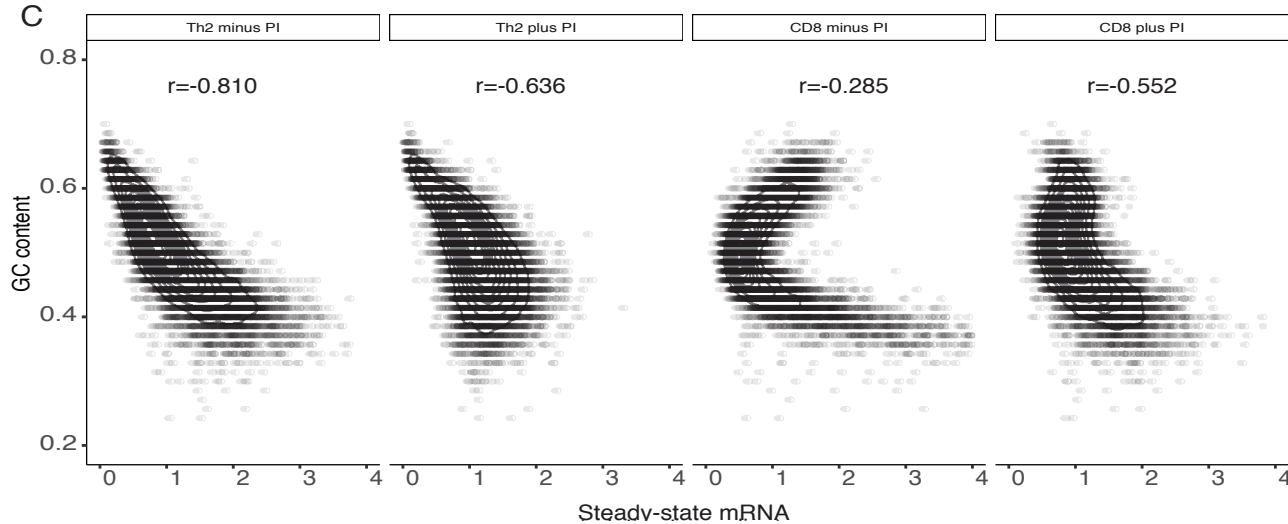
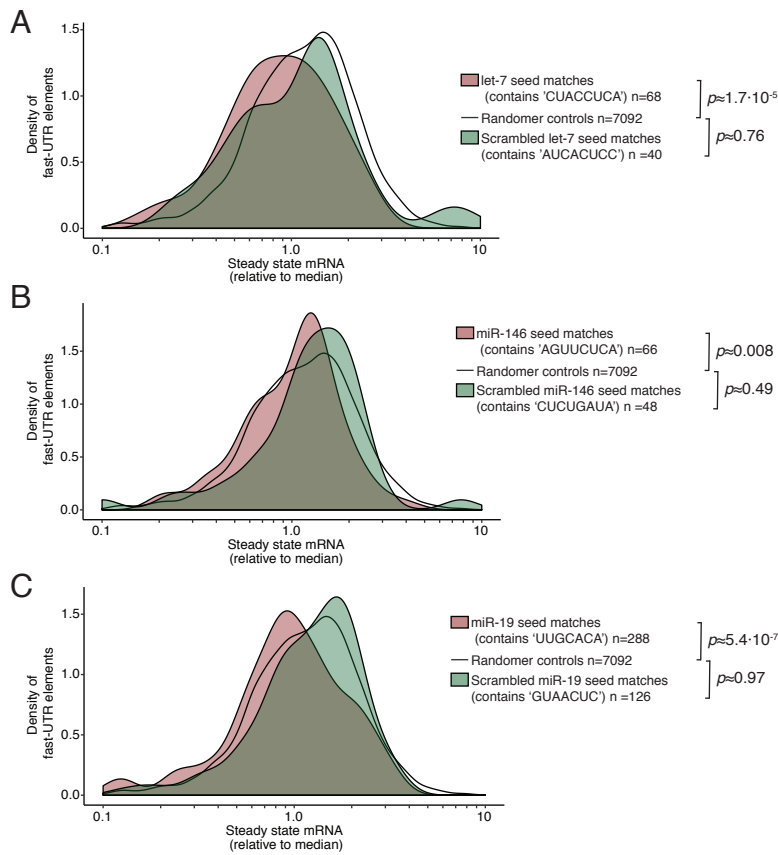
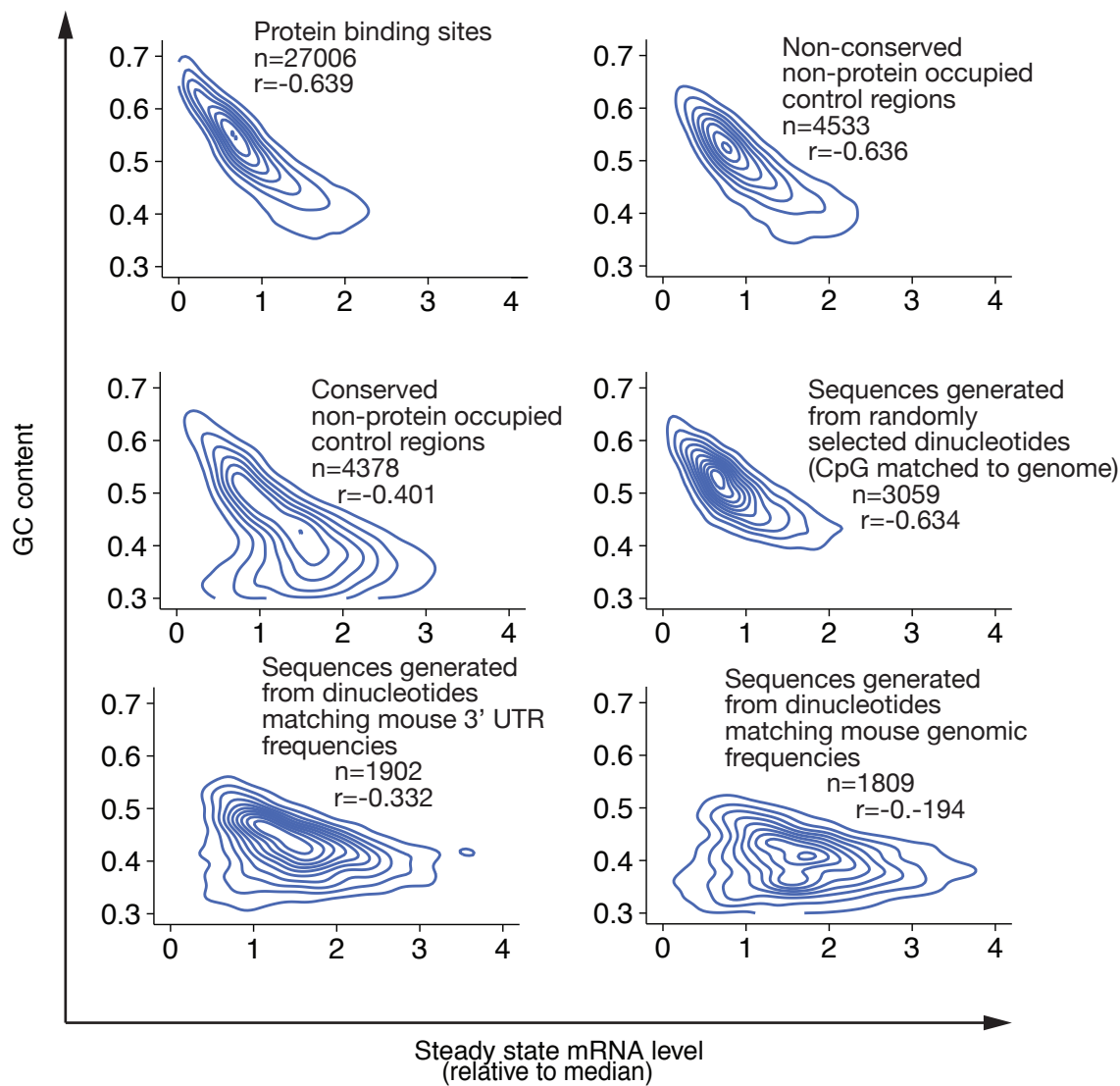


A**B****C**

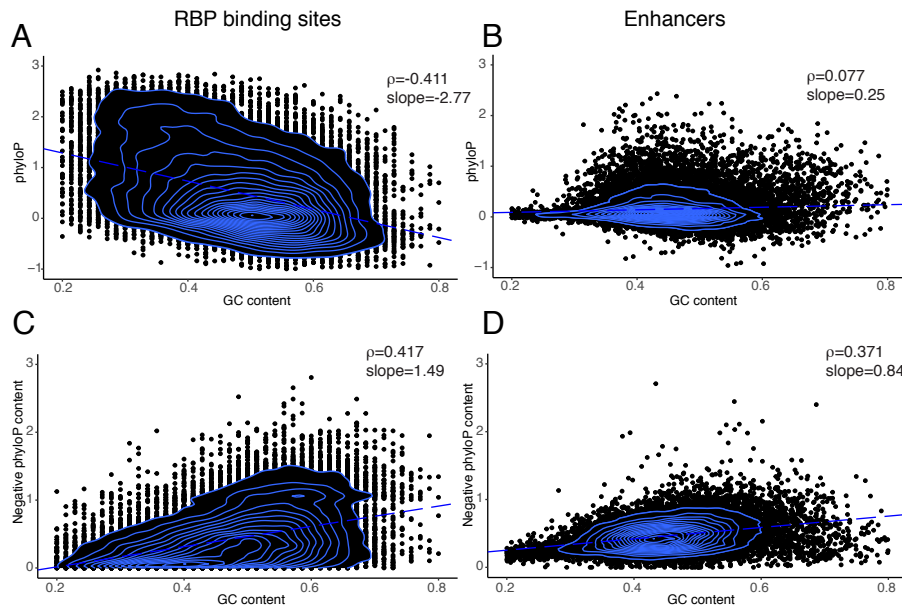
Supplemental Figure S1. Repeatability of Fast-UTR reporter assay. Steady-state mRNA abundance for all inserts in the fast-UTR library was determined in four total replicates in two biologically independent experiments. (A) Pearson correlation of steady-state mRNA level was calculated between pairs of samples for inserts present in all four replicates. (B) Bivariate plots show relationship between steady state mRNA level of individual library inserts across samples. Samples are arranged as in (A); r represents Pearson correlation. (C) Relationship between GC content and steady-state mRNA level for all four independent samples; r represents Pearson correlation.



Supplemental Figure S2. Sequences containing highly expressed miRNA seeds have lower mRNA abundance than scrambled controls in Fast-UTR reporter assay. Density plots showing median normalized steady-state mRNA abundance from the Th2 non-PMA/ionomycin stimulated sample for all inserts in the fast-UTR library containing specific miRNA seed sequences or indicated scrambled controls, shown against a background of all randomer control sequences (A) Let-7 seed containing sequences. (B) miR-146 seed containing sequences. (C) miR-19 seed containing sequences. Indicated p-values were calculated using Welch's two sample t-test.

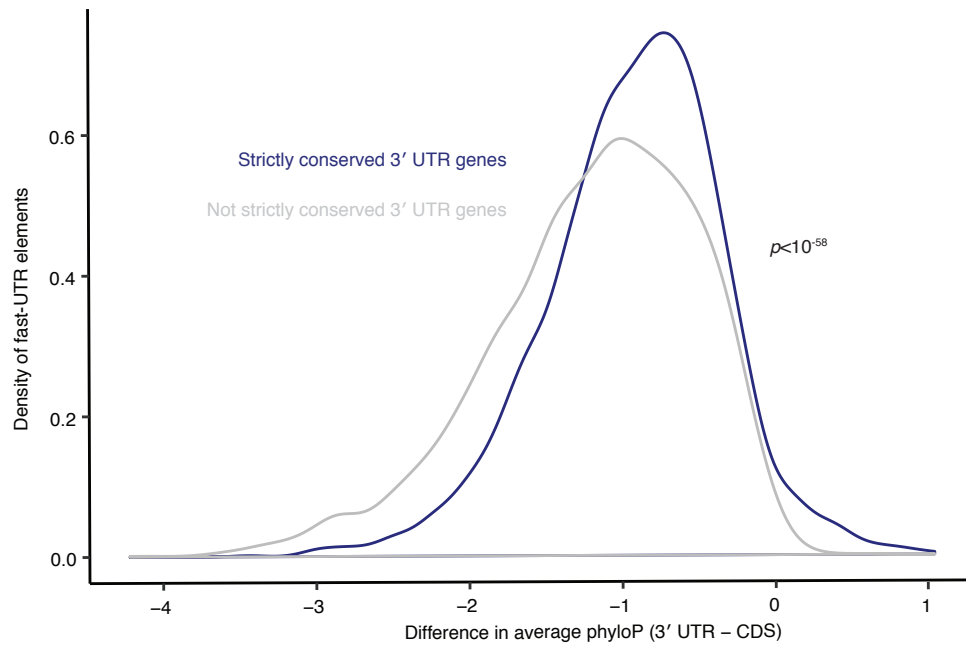


Supplemental Figure S3. Anti-correlation of steady-state mRNA and GC content across all tested classes of inserts. Correlation between GC content and steady-state mRNA level in inserts derived from RNA binding protein occupied sites in the mouse genome or 5 control classes of fast-UTR insert that varied widely in GC content. For each class, the number of inserts for which data were obtained (n) and the Pearson correlation coefficient (r) are indicated.



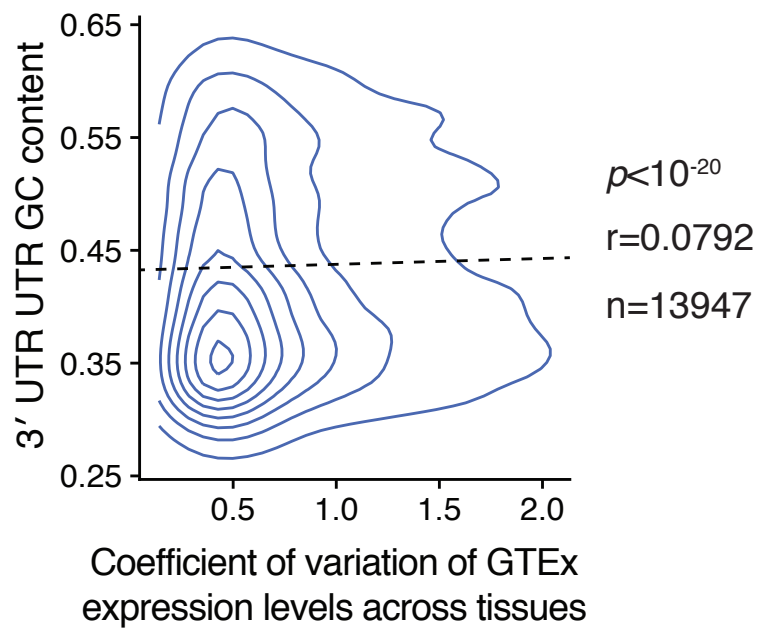
Supplemental Figure S4. RBP sites have greater selection on GC content than enhancers.

(A) and (B) Correlation between GC content and conservation (mean phyloP score) for (A) GCLiPP peaks and (B) EP300 peaks in Th2 cells. (C) and (D) Correlation between GC content and rapid evolution (negative phyloP content) for (C) GCLiPP peaks and (D) EP300 peaks in Th2 cells. In all panels, r represents Pearson correlation.



Supplemental Figure S5. Difference in conservation between coding sequence and 3' UTR.

For the classes of genes whose 3' UTRs were strictly conserved (dark blue) or not strictly conserved (gray, both defined as in Figure 6A) the difference in average phyloP score was determined between the 3' UTR and the coding sequence (e.g. a gene with the same average conservation score in the 3' UTR and the CDS would represent a 0 on this plot, -2 would indicate a higher conservation score in the CDS). p values represent Welch's unequal variance t-test of this difference between genes with strictly conserved and not strictly conserved 3' UTRs.



Supplemental Figure S6. Relationship of 3' UTR GC content and variability of gene expression across tissues. Correlation between GC content of the longest annotated 3' UTR of a given gene and its coefficient of variation across ~100 tissues as measured by RNA-seq in the GTEX consortium dataset. The number of genes indicated (n) and the Pearson correlation coefficient (r) are indicated.